Lidar-Derived Distribution of Cloud Vertical Location and Extent

A. I. CARSWELL, A. FONG, S. R. PAL, AND I. PRIBLUDA

Institute for Space and Terrestrial Science and Department of Physics and Astronomy, York University, North York, Ontario, Canada

(Manuscript received 13 December 1993, in final form 25 March 1994)

ABSTRACT

This paper summarizes the results of a statistical analysis of lidar-determined cloud geometrical properties measured during the 1989 and 1991 campaigns of the Experimental Cloud Lidar Pilot Study. Useful lidar descriptors are introduced to specify the bottom-, top-, and midcloud altitudes. These are used to describe the behavior of cloud vertical location and vertical extent during several months of observations using a dual wavelength (1064 and 532 nm) Nd:YAG lidar at Toronto. Frequency distributions of cloud height and cloud thickness are presented and the relationship of the lidar descriptors to cloud properties are discussed. These data are compared with other information on cloud geometry available in the literature.

1. Introduction

Clouds play an important role in the radiative transfer of the earth's atmosphere. Their characteristics determine the amount of solar radiation reflected into space and absorbed by the atmosphere and the surface of the earth. To arrive at accurate estimates of the radiation budget, global climate modeling studies must correctly include the effects of clouds. However, clouds vary widely in type and characteristics, and their properties are variable in both space and time. At present, clouds remain one of the least well-quantified constituents in current modeling activities (Browning 1990; Senior and Mitchell 1993).

Lidar measurements of clouds have shown considerable progress in the determination of the optical as well as physical properties of clouds. Lidar can provide cloud information over large volumes of the atmosphere with excellent spatial and temporal resolution (Carswell 1981; Platt et al. 1994). As a result there is now the possibility of using lidar cloud data obtained over extended time periods and in different geographical regions to provide a new and comprehensive picture of the properties and behavior of clouds. Such a database would provide information that would be very useful for the development of appropriate parameterization of cloud contributions in general circulation models.

Although many groups have made lidar cloud observations for a number of years, (including some routine use of laser ceilometers for cloud-base height determination) an extensive and coordinated collection of cloud data by lidar is not yet in progress. As an initial step in this direction, the Experimental Cloud Lidar Pilot Study (ECLIPS) campaign was initiated in 1988 by 14 international lidar groups (Platt 1988; Platt et al. 1994). The ECLIPS program involves the measurement of clouds from below with ground-based lidars simultaneously with their observation from above with the *NOAA-10* and *NOAA-11* satellites.

The main goal of this pilot study is to determine the extent to which lidar information can complement and enhance the value of the satellite data. However, the lidar dataset on its own can provide considerable new information on the physical and optical properties of the clouds.

Two ECLIPS measurement campaigns have been completed: phase 1 in the fall of 1989 and phase 2 in the summer of 1991. Each phase lasted for about six weeks. The lidar data have been collected and analyzed according to a uniform protocol and have been archived by the lidar group at National Aeronautics and Space Administration (NASA), Langley Research Center[1].

The lidar group of the Institute for Space and Terrestrial Science at York University has made numerous lidar measurements of clouds during both ECLIPS phases. A high-power lidar has been used to probe the atmosphere at altitudes up to about 90 km, and all of the cloud systems present during the measurement times have been measured by the lidar. Apart from those occasions in which very dense low clouds obscure higher clouds, the lidar is capable of detecting and measuring all of the clouds present.

Corresponding author address: Prof. Allan I. Carswell, Dept. of Physics and Astronomy, York University, 4700 Keele Street, North York, Ontario M3J 1P3 Canada.

[1] Contact: Dr. M. P. McCormick, NASA/Langley Research Center, Atmospheric Sciences Division, Hampton, VA 23681-0001.

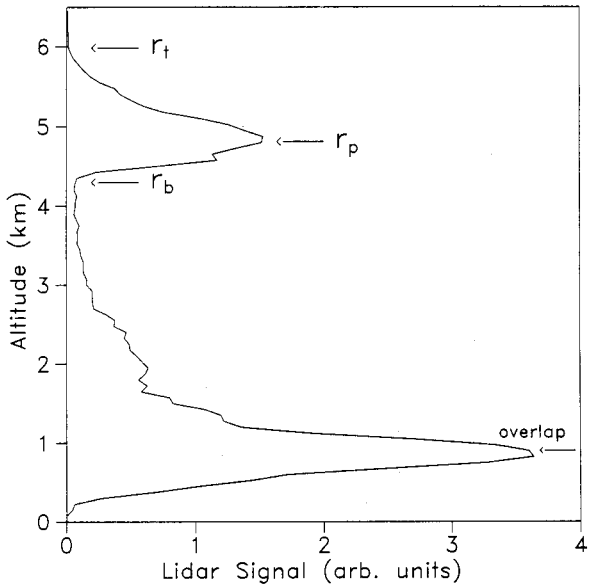

FIG. 1. Lidar backscatter return showing full pulse penetration. The heights of transmitter–receiver overlap, cloud bottom (r_b), peak (r_p), and top (r_t) are labeled.

The cloud property most easily measurable by lidar is the location and extent of the cloud. This is derived directly from the distribution of the cloud-induced enhancement of the back-scattered lidar signal above the signal from the ambient atmosphere. Analysis of the information content of the lidar signature (e.g., signal intensity, polarization, etc.) also provides information on some of the important optical properties of the clouds being probed.

In this paper the discussion is restricted to the first of these properties, namely, the location and vertical extent of the clouds observed during the ECLIPS program. The data for the entire measurement series are averaged to indicate the typical statistical properties of the clouds observed. In later papers, a summary of the findings on the optical properties of the clouds will be presented.

2. Lidar system and method

The lidar used for this work has a 20-Hz Nd:YAG laser transmitter, which provides a linearly polarized output at both 1064 nm in the infrared (IR) and 532 nm in the visible (Carswell et al. 1991). The lidar is a fixed, vertically pointing system with a receiver having dual-polarization measurement capabilities at both wavelengths. The backscatter signals at 532 nm are detected by photomultiplier tubes coupled to a photon counting system. The 1064-nm signals are detected by avalanche photodiodes coupled to high-speed A/D converters.

The minimum spatial resolution of the lidar along the beam is 75 m at 532 nm and 6 m for 1064 nm with the difference resulting from the different properties of the detection systems at the two wavelengths. Averaging of the signals over similar range intervals provides direct comparison of the returns at the two wavelengths. In the transverse direction, the spatial resolution is a function of distance as governed by the 0.3-mrad divergence of the lidar beam. Since the lidar pulses at the two wavelengths are transmitted simultaneously and the two beams are fully superimposed, the lidar is observing simultaneously the same cloud region at both wavelengths. Thus, even with rapidly changing cloud conditions, the two wavelengths are observing the same portion of the cloud. This aspect is important when intercomparing the resultant observations at the two wavelengths.

The full overlap of the receiver field of view with the transmitted beam occurs at an altitude of 825 m for 532 nm and 600 m for 1064 nm. Although corrections can be made to derive information at lower altitudes, in the current work no data below the overlap altitudes are used.

Typically, the lidar is fired continuously during a 3-h period centered on the satellite overpass time. The *NOAA-10* and *NOAA-11* satellites are polar orbiters and the typical overpass time was around 0800 or 1900 local time for *NOAA-10* and around 0330 or 1430 for *NOAA-11*. The measurements were made for all overpasses of both satellites where clouds were present. There were 37, 3-h lidar time series recorded in ECLIPS phase 1 (September–October 1989) of which 12 were during the day and 25 during the night. In ECLIPS phase 2 (June–July 1991) there were 22, 3-h time series of which 13 were during the day and 9 during the night.

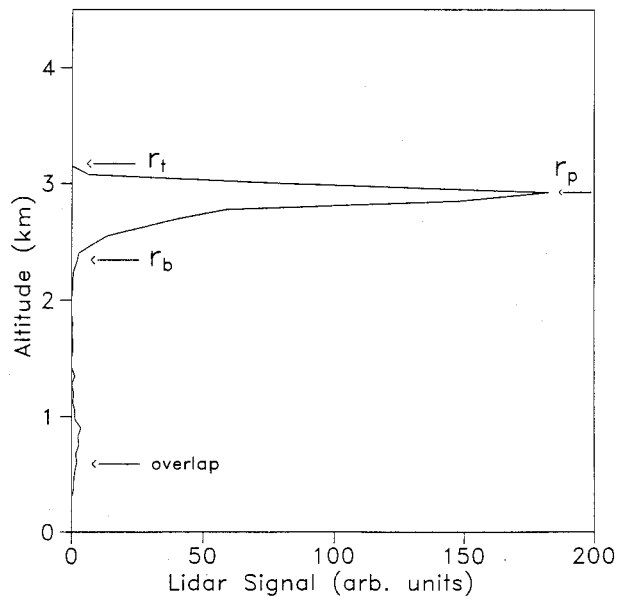

FIG. 2. Lidar backscatter return showing incomplete pulse penetration.

Since the number of cases during the day and night is quite limited, no attempt was made to study diurnal variation in cloud parameters.

The lidar pulse repetition rate was 20 Hz, and the returns at both wavelengths were hardware averaged for a 15-s interval (300 shots), then captured and stored on a dedicated PC that is coupled via Ethernet to a SUN system. Thus for a 3-h time period a maximum of 720 data points (15-s averages) could be obtained whenever there were clouds present. Since during the satellite overpasses the clouds were often broken, a typical run would provide fewer data points than this. The total number of data points before averaging, utilized for the analysis of this paper was in excess of 11 000 for each ECLIPS phase. Simultaneous time-lapse color video recordings are made with a coaligned camera. This information is then available if needed for later cloud-type identification or other applications. (Pal et al. 1994).

The ECLIPS archive requires time averages of the cloud parameters with a maximum duration of 10 min. Shorter than 10-min averages will result from the discontinuity in cloud layer. Although the lidar continues to observe the clear-sky profiles (during cloud discontinuity), these clear-sky profiles are not included in the averaging. Except for a heavy overcast when a cloud exhibits many successive full 10-min averages, it has been generally observed that breaks in a cloud are quite random, rendering averaging intervals of uneven duration. Since a 3-h run involves a large number of profiles with and without a cloud on them, our group developed an automated data analysis algorithm that took care of this aspect of cloud variability (Pal et al. 1992).

In this algorithm the averaging process is initiated when the lidar signal first detects the cloud. If the cloud is continuous the averaging interval would continue for the full 10-min period (involving 12 000 profiles) and then automatically reinitiate itself for another 10-min period and so on until the end of the time series is reached. In any 3-h period there would then be a series of such time intervals defined by the specific structure of the clouds occurring. Once these time intervals are determined all lidar returns within the interval are averaged and subsequently analyzed for retrieving the cloud parameters using the algorithm.

When averaging in the vertical direction to obtain spatial information on the cloud structure it is also necessary to exercise care not to mix separated cloud layers at different altitudes. The algorithm records separate sets of cloud parameters for separate cloud layers. These details are given in Pal et al. (1992). The vertical averaging is performed separately for separate layers.

3. Lidar cloud descriptors

In principle the most directly observable characteristic of clouds is their geometry—their physical location and vertical extent. In practice, however, because of their extremely irregular and time-dependent shapes, the determination of key geometric descriptors of clouds is a nontrivial task. Historically, cloud-base height and cloud-top height have been the principle descriptors in the vertical direction, whereas (fractional) cloud cover has been used as a rough indication of horizontal cloud extent. More recently, with the availability of aircraft- and satellite-based imagery the horizontal geometry of clouds can be much more quantitatively monitored.

Lidar detects the presence of clouds by their enhancement of the backscattering above the return from the ambient atmosphere. Because of its high spatial and temporal resolution, lidar can detect and locate clouds in three dimensions with a precision unmatched by any other sensor system. The shape, size, and location of the regions of enhanced scattering can usually be determined to within a few meters if desired. A problem does arise, however, in defining how to relate this optical discontinuity to the properties of clouds determined by other means.

An important example of this is the problem of selecting a definition of "cloud-base height" as determined by lidar that is compatible with cloud-base height definitions derived from other observational methods (e.g., visual sighting, ceilometers, etc.). This question has been addressed in an earlier paper (Pal et al. 1992). As discussed in that paper, the lidar returns readily show the cloud "bottom" height r_b, where the scattering begins to increase above the ambient atmosphere. The altitude r_p of the location of the maximum backscattered signal within the cloud is also readily determined from a lidar cloud profile. In this work r_p is taken as the peak value of the uncorrected (raw) lidar profile. No attempt is made to correct for attenuation or multiple scattering since to do so requires additional information on the cloud, which is not generally available. Since the lidar is pointing vertically there will be situations in which specular reflections will be obtained from clouds containing horizontally oriented ice crystals (Thomas et al. 1990). This will not cause any problems with the determination of r_b or r_p as long as the total backscatter signal is used.

The location of the cloud-top height is more difficult because in many dense clouds the lidar signal does not completely penetrate the cloud. However, an "effective" cloud-top height r_t can be defined at the altitude where the lidar signal reduces back to the subcloud value either because the pulse has been completely attenuated in the cloud or has penetrated through the cloud to the ambient air above. This r_t value will locate only the true cloud top when the lidar pulse penetration is complete. To obtain this r_t value, range-corrected values of the signals at r_b and r_t were compared.

As discussed by Pal et al. (1992), there is at present no agreement in the literature as to which of the lidar observables should be utilized to provide the formal lidar descriptors of clouds. For example, the location

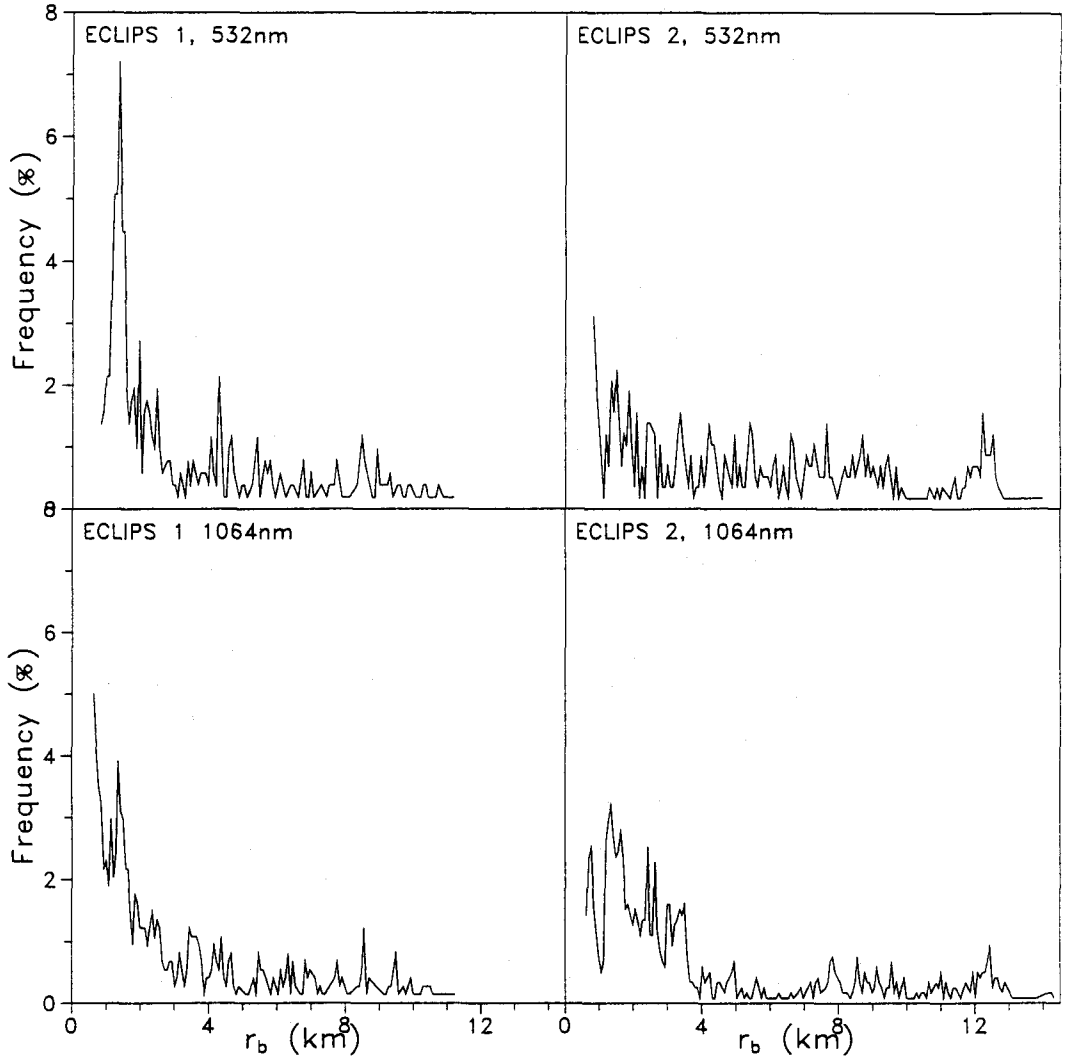

FIG. 3. Frequency distribution of cloud-bottom height r_b for ECLIPS 1 and 2 for measurements at 532 and 1064 nm.

of the cloud-base height is clearly somewhere between the altitudes r_b and r_p. But the exact definition of the location may well depend upon the application involved as indicated by Eberhard (1986).

Figure 1 shows a typical lidar profile. The altitudes of the "overlap" region, r_b, r_p, and r_t, are indicated. In this instance the overlap is complete by about 825 m and above that the signal in the ambient air generally decreases with altitude (being modulated somewhat by the variable content of aerosols in the lower atmosphere on this occasion) until it encounters the cloud. For such lidar profiles our algorithm automatically records the values of r_b, r_p, and r_t.

Figure 1 illustrates the case in which the lidar penetrates the cloud and provides a true indication of the location of the cloud top. In Fig. 2 a sample profile is shown for a situation in which a dense cloud fully attenuates the lidar signal within the cloud. In this case the r_t value indicates only the apparent cloud-top location.

In the analysis of our data it has been possible to identify relatively easily whether the lidar pulse has penetrated the cloud or not. This has been accomplished by utilizing the detailed features of the lidar signals available. For example, in Fig. 2 the large ratio of signal level at r_p to signal level at overlap is a clear indication of an extremely dense cloud layer. Also, the rapid and uniform exponential decay in the signal above r_p is a good indication that the signal is being completely attenuated within the cloud. Finally, because of the fact that the lidar is transmitting very large pulse energies (~0.5 J) at each wavelength, it is possible in most instances to measure the signal-to-noise ratio above r_t and identify those situations in which the signal has been fully attenuated.

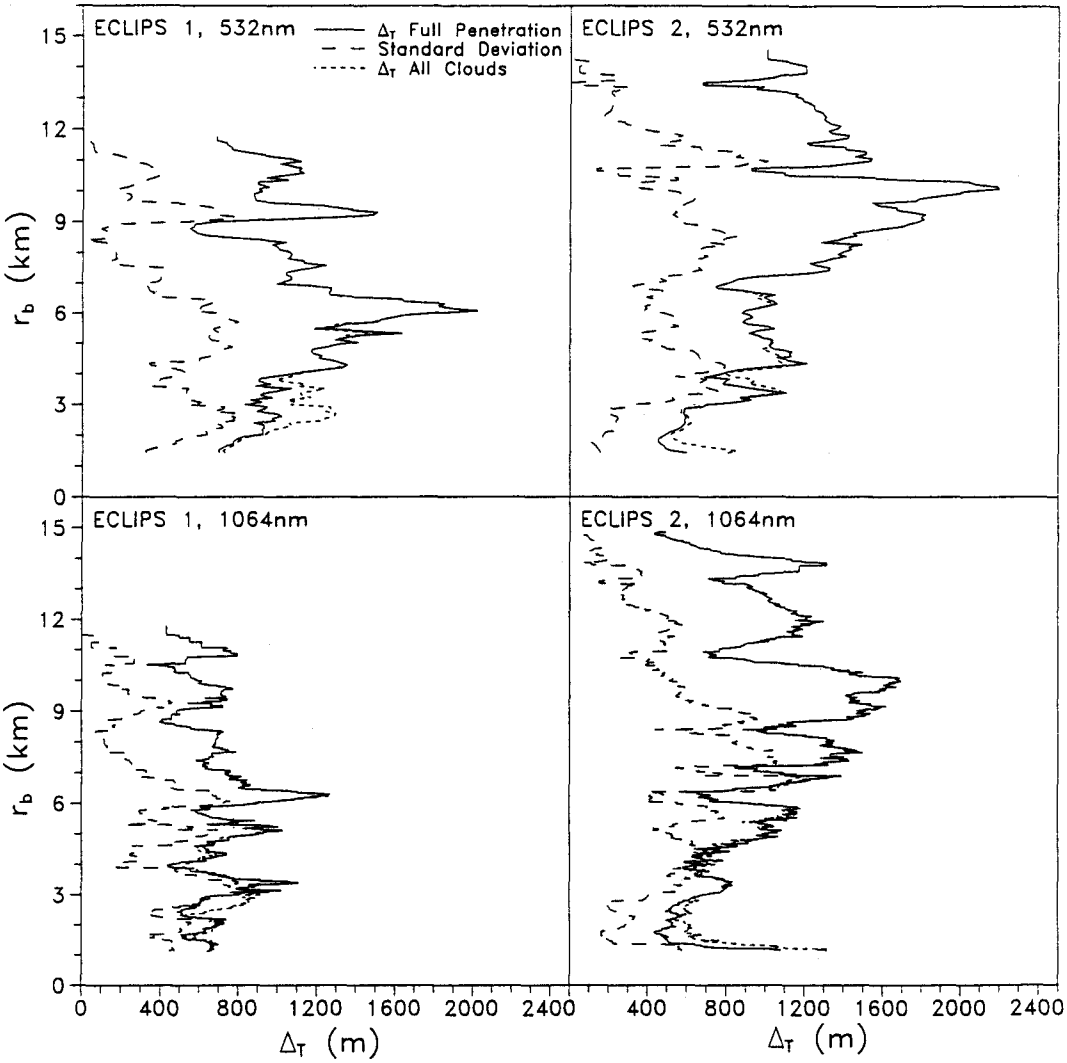

FIG. 4. Cloud thickness Δ_T variation with cloud-bottom height r_b for both ECLIPS phases and both wavelengths. The solid line is for clouds with "true" tops only. The dotted line includes clouds with apparent tops also. The standard deviation is shown by the dashed line.

It is recognized that on some occasions it is difficult to determine whether or not there has been full penetration by the pulse. However, for these ECLIPS data it has been possible to identify with good confidence those cases in which penetration was complete. These have been separated from the rest of the data for analysis involving r_t values. It was found that full penetration occurred for about 82% of the clouds in the ECLIPS phase 1 (September–October 1989) and for about 93% in phase 2 (June–July 1991). In the presentation of the data these cases have been treated separately so that the use of the r_t values in general indicates the location of the true cloud-top position.

Using the above descriptors, the cloud "thickness" can be defined as $\Delta_T = r_t - r_b$, where only the values of r_t for full penetration of the signal are used. In this paper all of the results are presented in terms of the lidar observables defined above. The potential value of these as formal cloud descriptors and their relationship to other cloud descriptors is discussed briefly in the paper. In the following sections the cloud properties measured during the two ECLIPS phases are presented.

4. Observations

a. Cloud height as defined by r_b

Figure 3 summarizes the cloud-bottom location r_b and the data for each wavelength and each ECLIPS phase are shown separately. In this figure all of the data are shown with a vertical resolution of 75 m. (The 1064-nm, 6-m resolution has been averaged over 75 m to allow more direct comparison with the information at 532 nm.) The mean sea level at the lidar site is 186 m

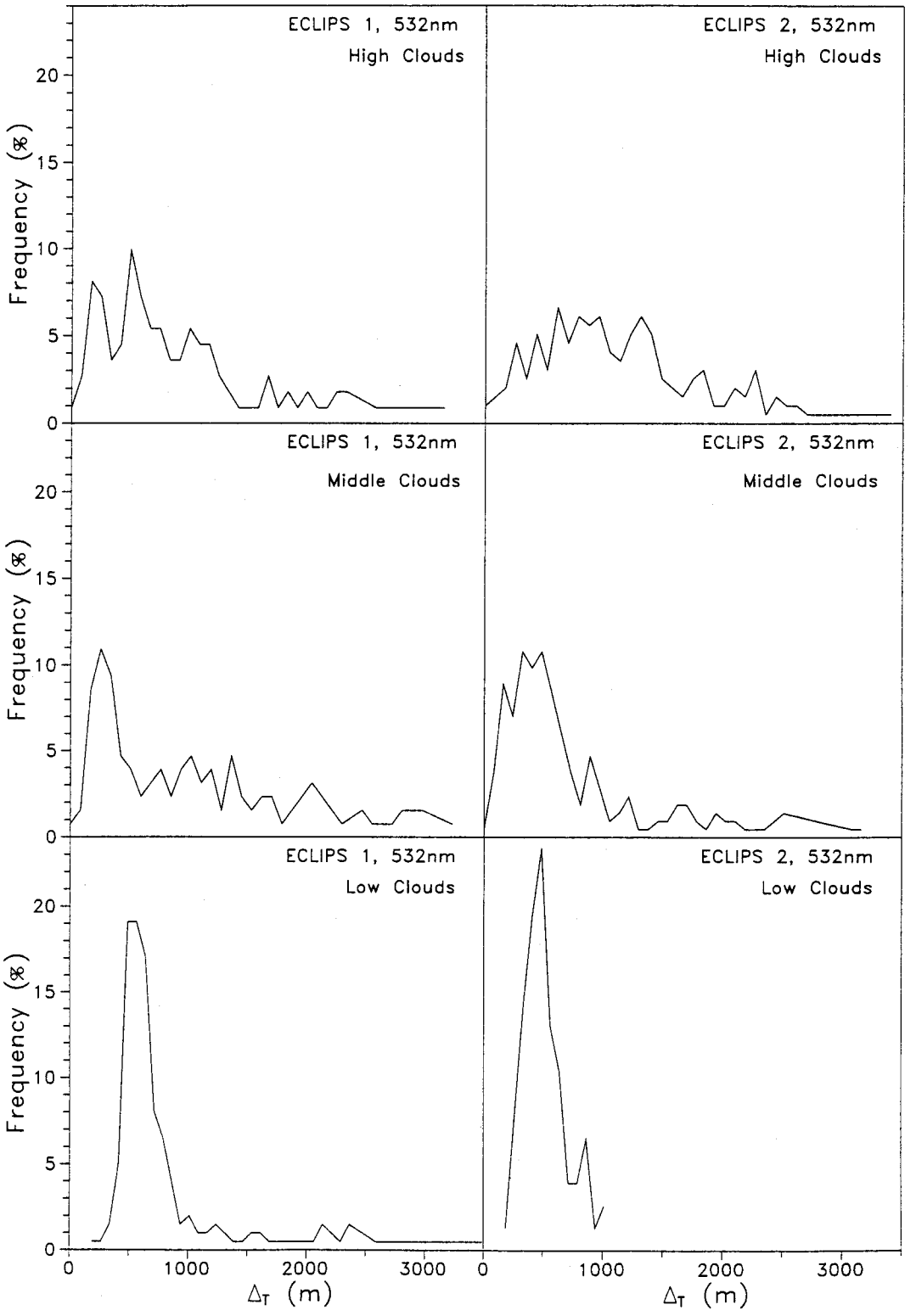

FIG. 5. Frequency distribution of cloud thickness.

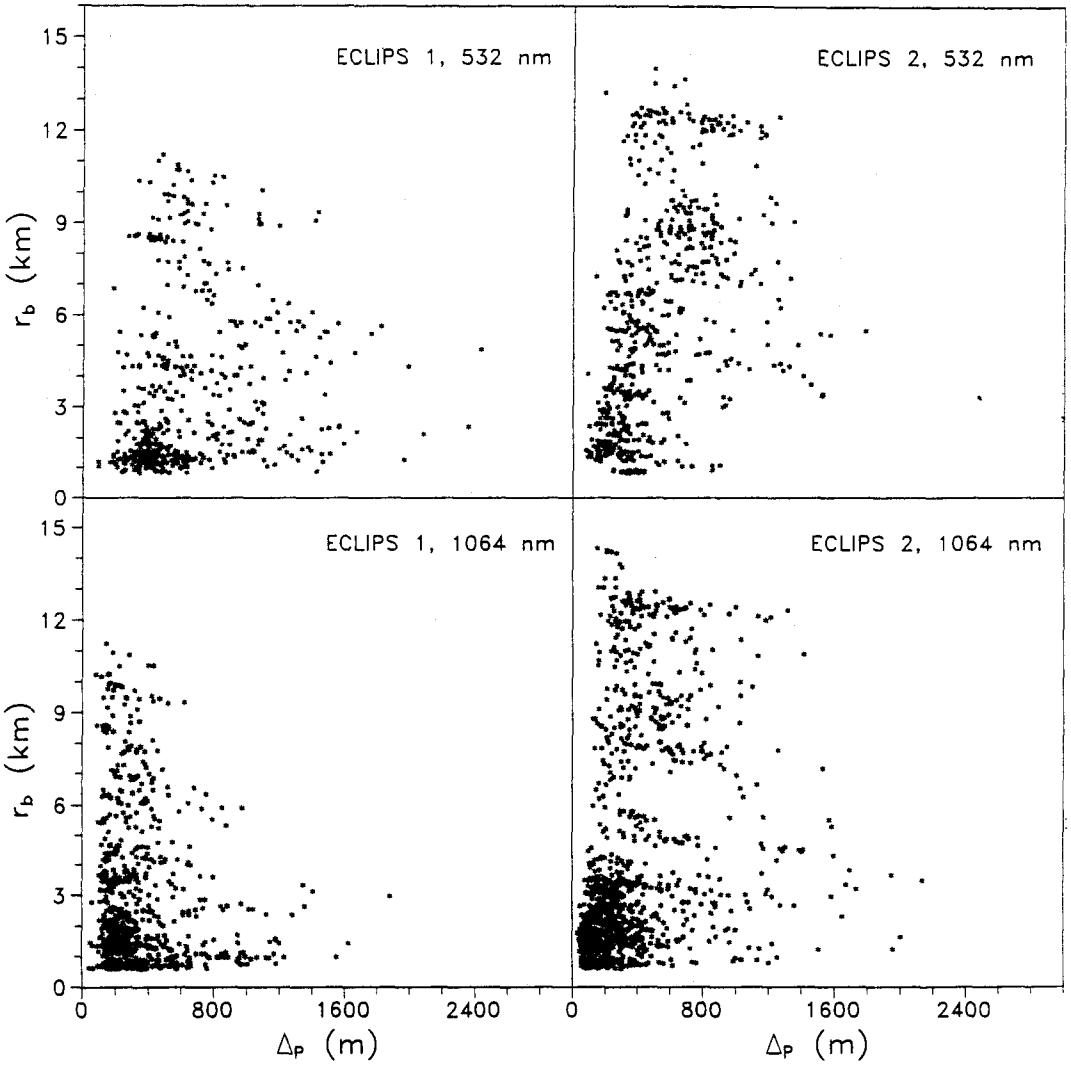

FIG. 6. The scatterplot of $\Delta_P = r_p - r_b$ with respect to cloud-bottom height.

and the cloud heights in this paper are above ground level.

Although the plots in Fig. 3 show sizable fluctuations, there is general agreement in the overall trend to higher probability of occurrence of cloud base at lower altitudes. In all cases the most probable altitude of occurrence of cloud bottom is 1–1.5 km. Phase 1 (September–October 1989) data show a greater frequency of low clouds, whereas phase 2 (June–July 1991) shows a higher occurrence of cirrus above 11 km. The higher tropopause height in the summer months and other seasonal differences could account for this. However, the phase 2 data were being collected shortly after the Mount Pinatubo volcanic eruption in June 1991. Our stratospheric lidar data show very large enhancements of the stratospheric aerosol layer at higher altitudes in this time period and the precipitation of some of this material into the upper troposphere could have provided an increase of condensation nuclei for high-altitude cloud formation. The aerosol layers and cirrus could be readily distinguished in the lidar returns because of their different optical properties.

Comparison of the plots shows general correspondence at the two wavelengths although there is considerable difference in the fine structure. This difference results from the different "sensitivity" of cloud detection at the two wavelengths. Mie calculations show that the cloud droplet backscattering and attenuation properties do not change much between the two wavelengths, but the scattering of the ambient molecular and small aerosol particles changes substantially. For example, at 1064 nm the ratio of cloud-to-molecular (Rayleigh) scattering is a factor of about 16 greater than at 532 nm. This means that in the infrared the cloud-induced scattering enhancement above the ambient atmosphere is much

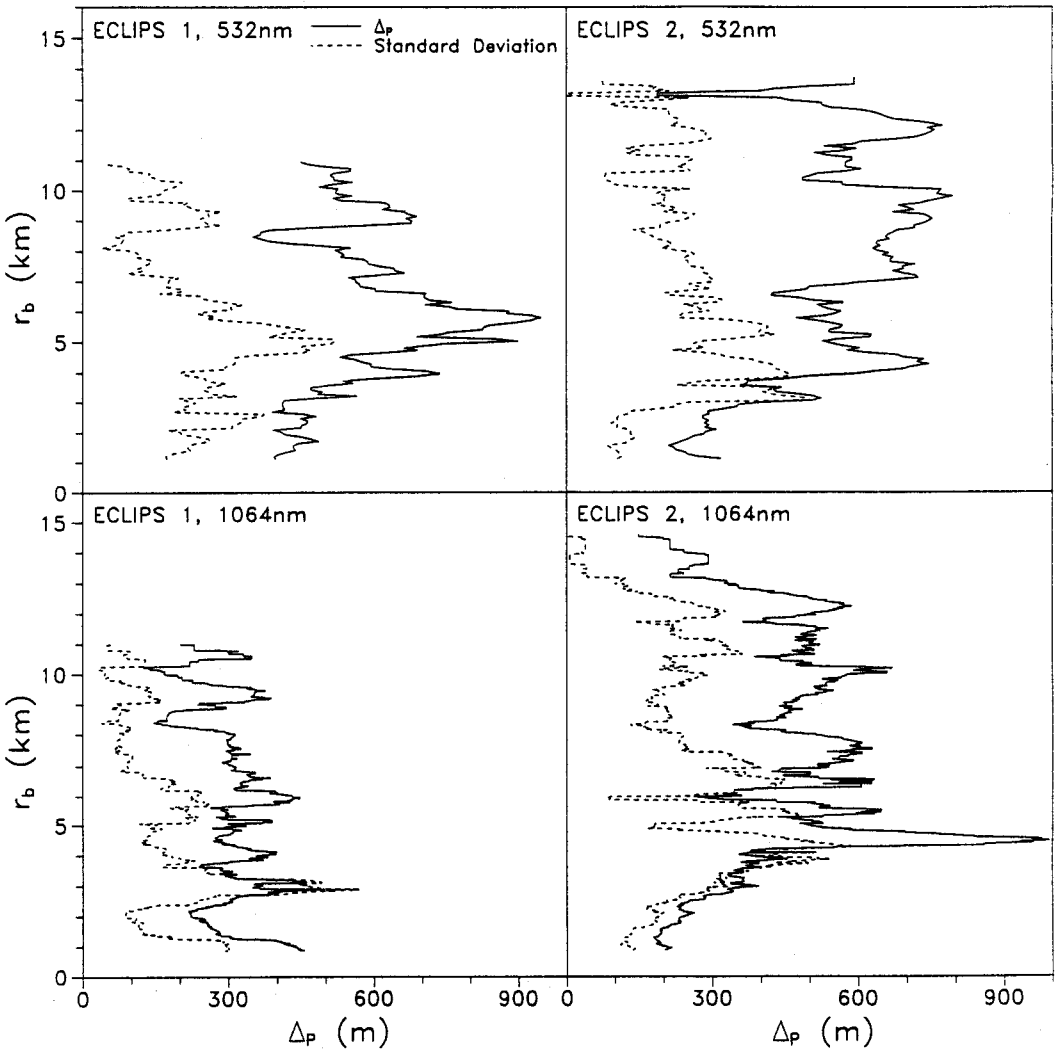

FIG. 7. Same data as in Fig. 6 with a sliding average over a height bin of 525 m. The dashed line represents the corresponding standard deviation.

greater than in the visible. As a result the 1064-nm lidar beam will detect and record more of the dilute and tenuous clouds than the 532-nm signal.

In addition, even though both datasets are averaged to a spatial resolution of 75 m, the IR will detect more of the physically very thin (less than 75 m) cloud layers than the visible because of the better (6 m) measurement resolution in the IR. Both of these factors tend to increase the number of clouds recorded in the IR channel. This is generally not a large increase, but this wavelength-dependent bias in cloud detection should be recognized in any statistical summary of cloud data. It is also recognized that there may be some obscuration of higher clouds by lower ones at both wavelengths, but for the current dataset this should not produce a substantial change in the distribution shown in Fig. 3.

b. Cloud thickness

The data on cloud physical thickness are shown in Fig. 4. In this figure the quantity, $\Delta_T = r_t - r_b$ is shown as a function of altitude (r_b) for both phases at both wavelengths. In this figure the data using the "true" r_t values (for which full penetration of the cloud has been achieved) have been plotted separately along with the data for the total set, which includes the thicknesses derived from the "apparent" r_t values as well. Also shown are the standard deviations for the total dataset.

In Fig. 4 there is no apparent dependence of cloud thickness on altitude. In fact, the two phases show considerably different thickness variation with altitude. In phase 1 the typical thickness lies between 1 and 1.5 km and is roughly independent of altitude. In phase 2 there is a trend of increasing thickness with altitude up to a height of about 10 km. The frequent occurrence

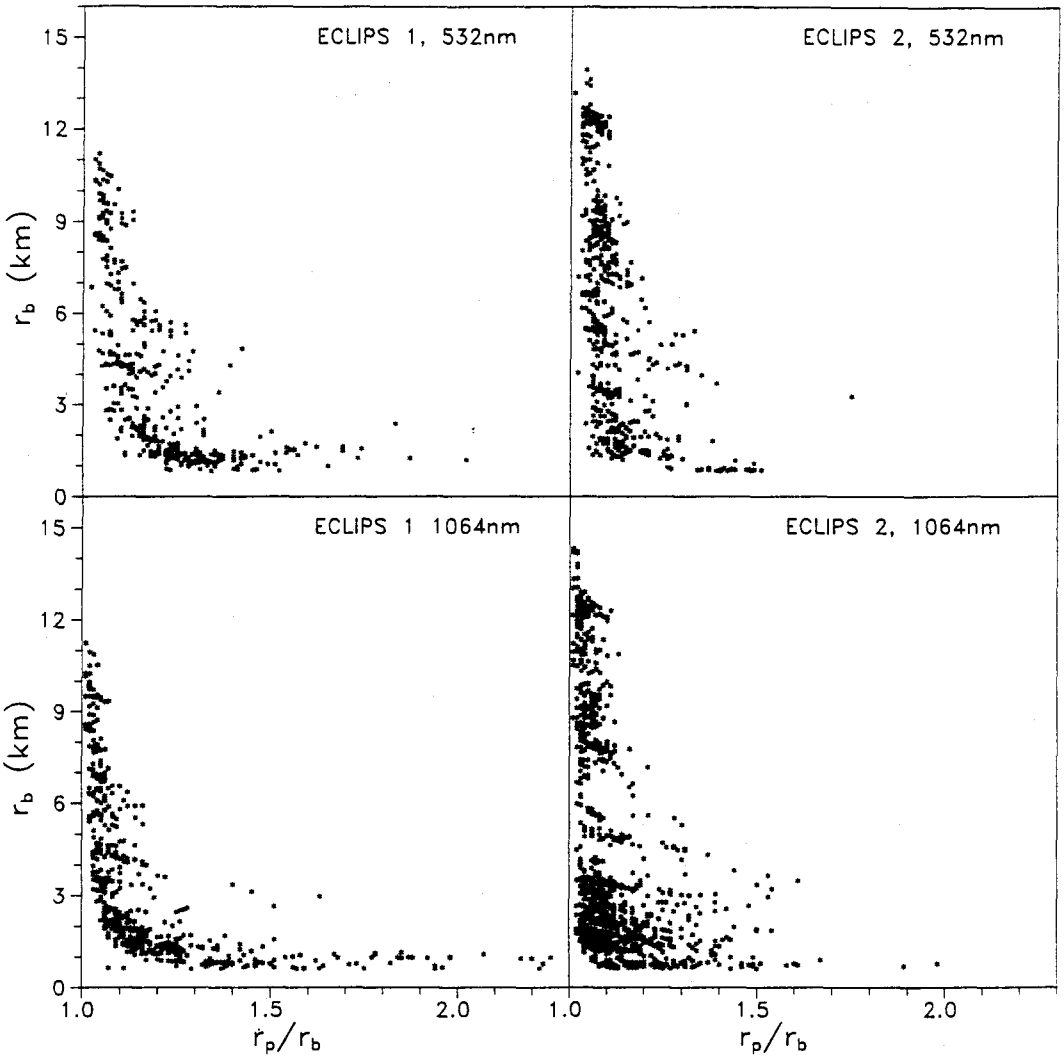

FIG. 8. The scatterplot of the ratio of cloud peak to bottom height as a function of cloud-bottom height.

in phase 2 of high (up to 15 km) cirrus clouds as mentioned above is also apparent.

In the ECLIPS 1 data of Fig. 4 there is a larger wavelength-dependent difference than for the ECLIPS 2 data. At present we have no explanation for this difference. The better range resolution of the 1064-nm data is also seen in the more detailed fine structure of the IR plots compared to the visible. In general the IR Δ_T values are less than the corresponding values in the visible, whereas the overall trends of the altitude dependences are similar.

The effect of including the apparent cloud-top data in Fig. 4 is seen only at low altitudes (dotted curves). As mentioned, full lidar beam penetration is not achieved for some of the optically dense low clouds. Including these cases in the dataset tends to increase slightly the observed thickness values at low altitudes. The problem of low dense cloud obscuration of higher layers can become serious in seasons and locales where such clouds are frequent and lidar pulse energies are unable to penetrate full cloud thickness. Above 3 or 4 km there is no difference in the data since all of the higher clouds were penetrated by the lidar. Thus for these data the error introduced by including the effective top height information is small.

It is seen from Fig. 4 that the statistical variation of the data is quite large even for the large dataset of many thousand samples. This merely reflects the fact that real atmospheric clouds have widely varying properties, and that even with a large number of observations the standard deviation is quite large.

In Fig. 5 the frequency of occurrence of cloud thickness in the visible has been plotted in the three World Meteorological Organization (1975) altitude classes (low: 0–2 km, middle: 2–7 km, high: 5–13 km). In this figure the data have a vertical resolution of 75 m. The

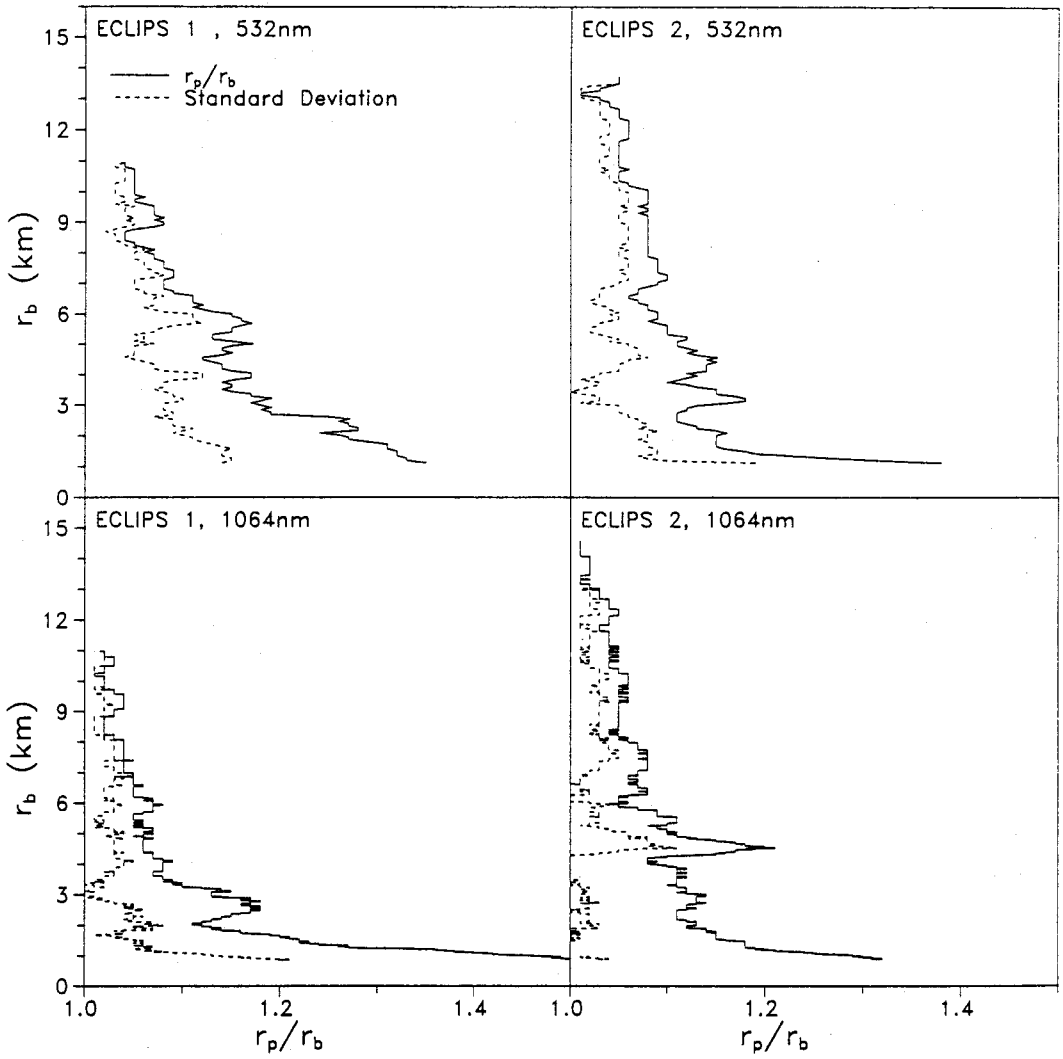

FIG. 9. Same data as in Fig. 8 with a sliding average over a height bin of 525 m. The dashed line shows the standard deviation.

low clouds show a rather narrow range of thicknesses localized around 500 m. For the high cirrus clouds a broader range is seen with thicknesses up to about 3 km with a most probable value of about 1 km. The middle clouds show a behavior that is more or less a superposition of the other two.

c. *Cloud height as defined by r_p*

As discussed above the lidar backscatter signal usually indicates quite well the transition at r_b between the subcloud aerosol and the cloud droplets. There are, however, some situations when this transition is not well defined such as in the presence of virga or when there are high concentrations of haze below the cloud boundary. In such cases the determination of r_b and hence the location of cloud-bottom height becomes indefinite. This is clearly a disadvantage if the lidar descriptor r_b were to be adopted as the formal definition of cloud (base) height.

For any cloud layer the height of the lidar backscatter signal maximum r_p can always be determined unambiguously since it is simply defined as the altitude of the peak signal return. Thus r_p could be utilized as an alternative designator of cloud height that is readily measured by lidar. Although it is clear that r_p always lies between r_b and r_t, its exact location will depend upon the optical and geometrical properties of the specific cloud. In an effort to determine how the location of r_p relates to the other geometric properties of a cloud, the ECLIPS data have been summarized below in terms of the location of r_p within the clouds observed to date.

Figure 6 shows a scatterplot of the variation of $\Delta_p = r_p - r_b$ as a function of the cloud-bottom height r_b. Here Δ_p indicates the distance in meters that the observed peak signal r_p lies above the cloud-bottom lo-

cation r_b. The scatterplot includes all of the measurements and has been used to show more clearly the distribution of the data points. In Fig. 7 average profiles for these data have been generated using a sliding height bin of 525 m. The standard deviation about this average is also shown in Fig. 7.

Overall, Figs. 6 and 7 do not indicate any height-dependent variation of Δ_p. There is the trend to smaller values in the IR than in the visible, particularly in phase 1 where the Δ_p (IR) is about 300–400 m and Δ_p (vis) is 500–600 m. In phase 2, Δ_p (IR) is about 500–600 m and Δ_p (vis) is about 600–700 m. This difference arises from the different scattering and attenuation at the two wavelengths and the instrumental effects described earlier. As in Fig. 4, the data in Fig. 7 show large standard deviations arising from the variable nature of the clouds observed.

The relatively height-independent behavior of Δ_p shows that as the height of a cloud increases, the relative difference between r_b and r_p as cloud height designators diminishes. This is shown in Figs. 8 and 9 where the ratio r_p/r_b is plotted as a function of r_b. Figure 8 shows the scatterplot of all data and Fig. 9 the average profiles along with the standard deviations.

It is seen from the figures that in all the data the ratio r_p/r_b decreases rapidly with altitude falling in most cases to values less than 1.1 at altitudes above about 3 km. For many applications this means that for clouds above this altitude r_b and r_p are virtually equivalent as the cloud height designator since there is a difference of less than 10% in their relative cloud height values. For cirrus clouds this difference is generally less than 5%. However, for low clouds the relative difference between the two can be greater than 50%.

The more specific location of r_p within the cloud can be obtained by comparing the distance Δ_p of the peak signal above the cloud bottom with the full thickness Δ_T of the cloud. This has been done for the ECLIPS

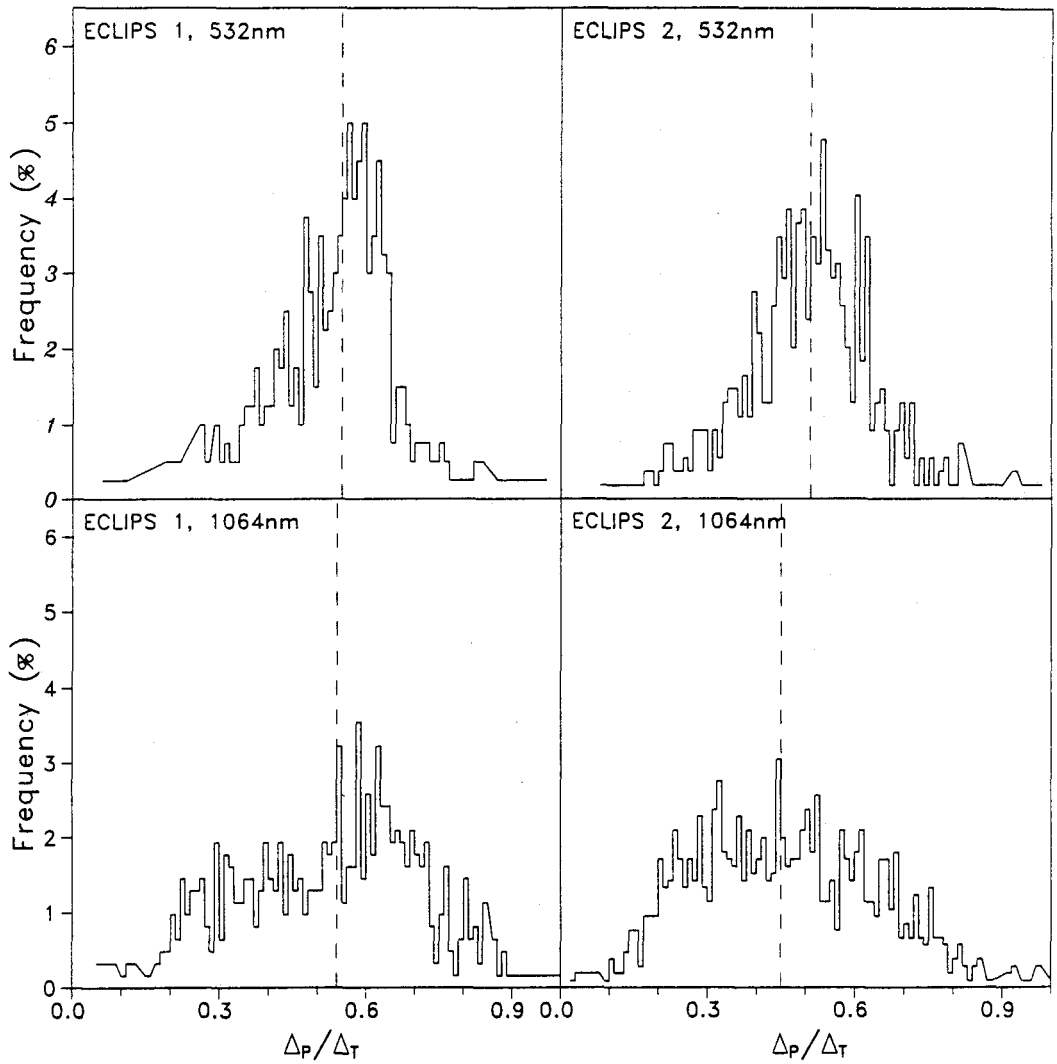

FIG. 10. Frequency distributions of the ratio Δ_P/Δ_T showing the relative location of the peak signal within the cloud.

dataset in Fig. 10. In this figure histograms of the frequency of occurrence of the ratio Δ_p/Δ_T are shown for both phases and wavelengths. The dotted lines indicate the centroids of the distributions.

Although the four distributions differ considerably in detail, they all exhibit a centrally peaked shape indicating that the most probable location of r_p is near the middle of the cloud. For phase 1 the specific values of the centroids are 0.55 and 0.54 for the visible and the IR, respectively. For the phase 2 the corresponding values are 0.51 and 0.45. The IR centroid is slightly lower than the corresponding value in the visible. These values indicate that on average the lidar observable r_p at either wavelength could serve very well as a descriptor for the midcloud height.

5. Comparison with other measurements

Although clouds have been studied for a long time and their parameters have been assessed and utilized in numerical schemes, very few measurements have been published that describe quantitatively the actual behavior of their geometrical or optical parameters. Even the large dataset of cloud-base height information being generated by current ceilometer networks has not been generally used for much more than short-term local applications.

Since cloud characteristics are dependent on local geographic and seasonal conditions, it is not easy to make meaningful comparisons between measurements made at different sites. Another difficulty in such comparisons arises from the differences in the measurement techniques employed to derive cloud parameters. As pointed out by Eberhard (1986), the different techniques do provide different cloud geometrical parameters. In addition as indicated in an earlier publication

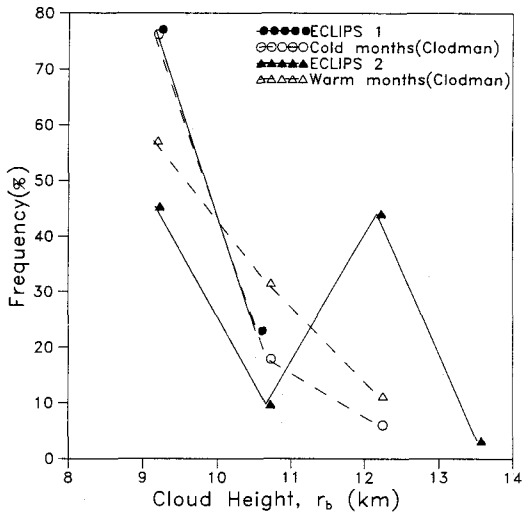

FIG. 11. A comparison of the frequency distribution of cirrus cloud heights measured by lidar with those of Clodman (1957).

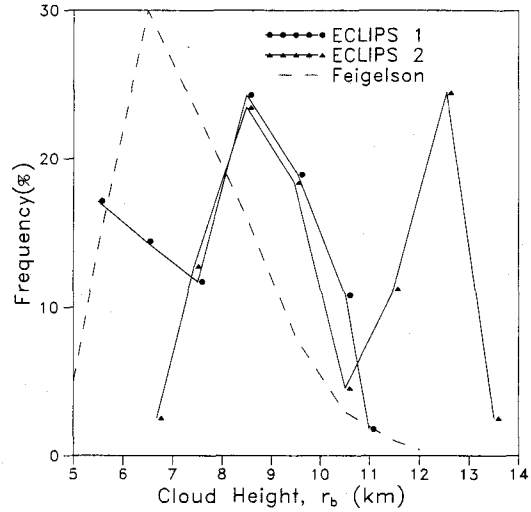

FIG. 12. As in Fig. 11 but comparing with the data of Feigelson (1984).

(Pal et al. 1992), a number of the important cloud descriptors are ill defined or are operationally defined in terms of a particular measurement method. Averaging procedures as well may vary considerably to further complicate attempts at comparisons.

With these limitations in mind, the lidar-based ECLIPS measurements have been compared with some existing information available from other measurements. The comparisons are quite limited because of the lack of suitable published information in the literature. In several instances it has been necessary to reformat the published data to permit a more direct comparison with the lidar information.

Clodman (1957) has analyzed over 2000 reports from Royal Canadian Air Force pilot observations of cirrus clouds. He has concluded that in the Canadian latitude zone the distribution in the months of June–September showed an average cirrus thickness of about 1.5 km with average cloud base of about 8.7 km.

The average values of these parameters in our lidar measurements during June and July (phase 2, Fig. 5) give an average thickness value of 1.5 km and an average base height r_b of 10.0 km. Clodman's data during intermediate months (March, April, May, and October), which relate to some extent to phase 1 (September and October), indicate values of these parameters to be about 1.4 and 7.8 km. As compared to these, the phase 1 lidar measurements give a mean value of cloud thickness to be 1.2 km and the cloud base to be 8.1 km.

The International Cirrus Experiment was conducted simultaneously with ECLIPS phase 1 during September–October 1989 over Europe (Boesenberg et al. 1990). This work, utilizing ground-based and airborne lidars, concluded that the average Δ_T and r_b values for the 38 cirrus cases observed were about 1.6 and 9.1

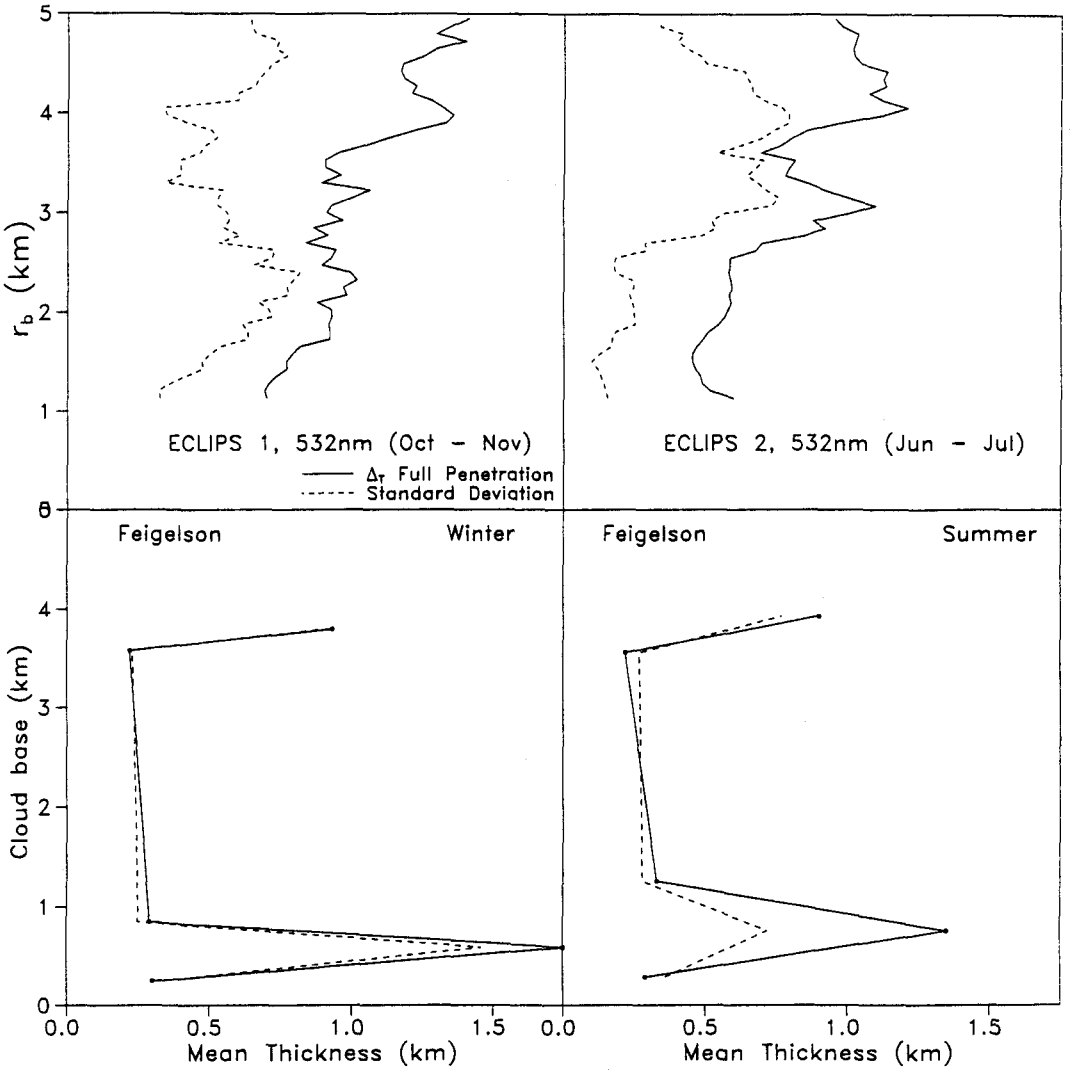

FIG. 13. A comparison of cloud thickness variation with cloud height for low clouds measured with lidar and by pilot observations (Feigelson 1984).

km, respectively. Our average cirrus values for these same parameters are 1.2 and 8.1 km (Figs. 3 and 5). As seen from these figures, however, the utility of the simple average value is somewhat questionable in view of the wide variation in the actual values of these parameters.

A comparison is possible between the lidar-derived frequency of occurrence of r_b and the aircraft observations of cloud-base height reported by Clodman (1957) for cirrus clouds. For this comparison the fine structure (75-m resolution) in the lidar data of Fig. 3 has been converted to match his range bin of 5000 ft (1.5 km) and it is assumed that the visually observed base-height value is equivalent to the lidar r_b. This comparison is shown in Fig. 11. Overall the data matches relatively well (considering the large differences in methodology and time) apart from the strong enhancement in the lidar phase 2 data, which introduces a secondary maximum at 12 km. As discussed earlier, this could be a result of the effects from the Mount Pinatubo eruption in 1991.

Feigelson (1984) summarized the frequency distribution of cloud-base height with 1-km range bin for cirrostratus (Cs) clouds from over 2000 daytime aircraft soundings over Moscow during 1957 to 1963. These data are shown in Fig. 12 by the dotted curve. The frequency distributions with 1-km range resolution were also determined for all clouds of cirrus and Cs nature from the ECLIPS measurements and these are presented in Fig. 12 for the two phases by the solid lines. Both the lidar and Feigelson's data show a maximum in this distribution; the lidar maximum being near 8.5 km and Feigelson's being near 6.5 km. Otherwise there is little correspondence between the two

sets of data. Once again the secondary maximum above 12 km in the phase 2 data is an unusual occurrence not present elsewhere.

Feigelson's work has also provided some comparative information on low clouds. A comparison between the observed cloud thickness Δ_T and its standard deviation for low clouds, derived from lidar and those tabulated by Feigelson, is provided in Fig. 13. Although the lidar data are not available below about 850-m altitude, this comparison shows very little correspondence between the two datasets. The greater resolution and information content of the lidar data is clearly evident. However, both datasets emphasize the great variability of cloud properties mentioned earlier. In both sets of observations the standard deviations in the measurements are of the same order of magnitude as the quantities being measured.

6. Conclusions

It is recognized that the data presented here are quite limited in scope. They are relatively sparse and are obtained only at a single location for rather limited time intervals. However, the analysis of this initial pilot study data demonstrates the valuable information on cloud geometry that can be obtained from lidar measurements. In addition the information base could be readily extended by applying similar analyses to the additional data already in the existing ECLIPS data archive at NASA Langley. The excellent space and time resolution of lidar measurements as well as the ability to measure a wide range of clouds from the ground are capabilities not matched by other sensor systems.

This work indicates a need to address the understanding and definition of the appropriate descriptors of cloud properties. Lidar has the potential to provide a much better quantification of cloud geometrical properties than are being used currently, either in modeling or in operational monitoring activities. To exploit this capability it will be necessary to define and agree upon a common and useful set of descriptors. These could then be used to assemble the extended database required for wider use.

In this work it has been found that to specify cloud vertical geometry the parameters r_b, r_p, and r_t are useful descriptors that are readily available from the lidar backscattered signal. These parameters can be easily obtained with any cloud lidar system. The principal limitation is in the determination of r_t for optically thick clouds. For the current ECLIPS data, however, such cases constituted a small subset of the clouds observed, and even when they did occur it was possible to identify them from the information contained in the lidar signal. In a subsequent paper we will be presenting an analysis of cloud optical parameters derived from the same ECLIPS data used in this paper.

Acknowledgments. The lidar research at the Institute for Space and Terrestrial Science is financially supported by the Ontario Premier's Council Technology Fund, the Atmospheric Environment Service and the Natural Sciences and Engineering Research Council of Canada. The authors express their appreciation to the other members of the lidar group who contributed to the ECLIPS measurement program.

REFERENCES

Boesenberg, J., A. Ansmann, S. Elouragini, P. H. Flamant, K. H. Klappheck, H. Linne, C. Loth, L. Menenger, W. Michaelis, P. Moerl, J. Pelon, W. Renger, W. Riebesell, C. Senff, P.-Y. Thro, U. Wandinger, and C. Weitkamp, 1990: Measurements with lidar systems during the International Cirrus Experiment 1989. Report No. 60, Max Planck Institute for Meteorology, Hamburg, Germany, 152 pp.

Browning, K. A., 1990: Rain, rainclouds and climate. *Quart. J. Roy. Meteor. Soc.*, **116,** 1025–1051.

Carswell, A. I., 1981: *Laser Measurements in Clouds: Their Formation, Optical Properties, and Effects.* P. Hobbs and A. Deepak, Eds., Academic Press, 363–406.

——, S. R. Pal, W. Steinbrecht, J. A. Whiteway, A. Ulitsky, and T. Y. Wang, 1991: Lidar measurements of the middle atmosphere. *Can. J. Phys.*, **69,** 1076–1086.

Clodman, J., 1957: Some statistical aspects of cirrus cloud. *Mon. Wea. Rev.*, **85,** 37–41.

Eberhard, W. L., 1986: Cloud signals from lidar and rotating beam ceilometer compared with pilot ceiling. *J. Atmos. Oceanic Technol.*, **3,** 499–512.

Feigelson, E. M., 1984: *Radiation in the Cloudy Atmosphere.* D. Reidel Publishing, 293 pp.

Pal, S. R., W. Steinbrecht, and A. I. Carswell, 1992: Automated method for lidar determination of cloud-base height and vertical extent. *Appl. Opt.*, **31,** 1488–1494.

——, I. Pribluda, and A. I. Carswell, 1994: Lidar measurements of cloud-tracked winds. *J. Appl. Meteor.*, **33,** 35–45.

Platt, C. M. R., 1988: Experimental Cloud Lidar Pilot Study (ECLIPS). Report, *WCRP/CSIRO, Cloud Base Measurement Workshop,* Mordialloc, Australia, CSIRO, Division of Atmospheric Research, 15 pp.

——, S. A. Young, A. Carswell, S. Pal, M. P. McCormick, D. M. Winker, M. DelGuasta, L. Stefanutti, W. Eberhard, M. Hardesty, P. Flamant, R. Valentin, B. Forgan, G. Gimmestad, H. Jäger, S. Khmelevtsov, I. Kolev, B. Kaprieolev, Darren Lu, K. Sassen, V. Shamanaev, O. Uchino, Y. Mizuno, U. Wandinger, C. Weitkamp, A. Ansmann, and C. Wooldridge, 1994: The Experimental Cloud Lidar Pilot Study (ECLIPS) for cloud-radiation research. *Bull. Amer. Meteor. Soc.*, **75,** 1635–1654.

Senior, C. A., and J. F. B. Mitchell, 1993: Carbon dioxide and climate: The impact of cloud parameterization. *J. Climate,* **6,** 393–418.

Thomas, L., J. C. Cartwrite, and D. P. Wareing, 1990: Lidar observations of the horizontal orientation of ice crystals in cirrus clouds., *Tellus,* **42B,** 211–216.

World Meteorological Organization, 1975: *International Cloud Atlas. Vol. I, Manual on the Observations of Clouds and other Meteors,* WMO, WMO-No. 47, 212 pp.